ISSN 1063-7826, Semiconductors, 2015, Vol. 49, No. 12, pp. 1582–1586. © Pleiades Publishing, Ltd., 2015.
Original Russian Text © A.R. Tuktamyshev, V.I. Mashanov, V.A. Timofeev, A.I. Nikiforov, S.A. Teys, 2015, published in Fizika i Tekhnika Poluprovodnikov, 2015, Vol. 49, No. 12, pp. 1630–1634.

XIX SYMPOSIUM "NANOPHYSICS AND NANOELECTRONICS", NIZHNY NOVGOROD, MARCH 10–14, 2015

Initial Growth Stages of Si–Ge–Sn Ternary Alloys Grown on Si (100) by Low-Temperature Molecular-Beam Epitaxy

A. R. Tuktamyshev*, V. I. Mashanov, V. A. Timofeev, A. I. Nikiforov, and S. A. Teys

Rzhanov Institute of Semiconductor Physics, Siberian Branch, Russian Academy of Sciences, Novosibirsk, 630090 Russia

**e-mail: tuktamyshev@isp.nsc.ru*

Submitted April 22, 2015; accepted for publication May 12, 2015

Abstract—Temperature dependence of the critical thickness of the transition from two-dimensional to three-dimensional growth of the $Ge_{1-5x}Si_{4x}Sn_x$ films grown on Si (100) by molecular-beam epitaxy in the temperature range 150–450°C has been experimentally determined. This dependence is nonmonotonic and is similar to that of the critical thickness for the transition from two-dimensional to three-dimensional growth in the case of the deposition of pure Ge on Si (100) and is caused by a change in the mechanism of two-dimensional growth. Data on the average size and the density of islands, and the ratio between the height of the islands and their lateral size are obtained by the methods of atomic force microscopy and scanning tunneling microscopy. As the growth temperature is increased from 200 to 400°C, the average size of the nanoislands increases from 4.7 to 23.6 nm.

DOI: 10.1134/S1063782615120222

1. INTRODUCTION

The microelectronic and optoelectronic applications of materials from Group IV of the periodic Table are limited due to a mismatch between the lattice constants of elemental semiconductors Si, Ge, and of their compounds, and also due to a small shift of the conduction band as a result of a variation in the composition in heterojunctions for these materials. Attempts directed at attaining the ability to independently control the band gap and strain caused by differences between the lattice parameters of the film and those of the substrate stimulated efforts toward the development of new semiconductor compounds.

Recently, ternary Si–Ge–Sn solutions have been studied. They feature interesting electronic and transport properties. In particular, independent control of the band gap and the lattice parameter was demonstrated in the family of ternary compounds Si–Ge–Sn, the lattice parameter of which coincides with that of elemental Ge [1, 2]. These data were obtained first for Group-IV semiconductors and made it possible to fabricate new optoelectronic devices compatible with silicon technology and covering the range of applications from communications [3–6] to high-efficiency solar cells [7]. In addition, due to a decrease in the band gap, the optical sensitivity of *p–i–n* photodetectors based on GeSn compounds is increased in comparison with germanium detectors [8]. Some studies have indicated that Si–Ge–Sn compounds can behave as direct-gap semiconductors [9, 10].

Epitaxial growth of $Si_xSn_yGe_{1-x-y}$ semiconductor compounds is complicated by the difference between the lattice constants of Sn and Ge (15%), Sn and Si (19%), by the low equilibrium solubility of Sn in Si and Ge (< 1%), and also by the instability of the diamond-like structure of α-Sn and the tendency to Sn surface segregation [11]. However, using nonequilibrium methods for growth, for example, low-temperature molecular-beam epitaxy (MBE), it is possible to grow single-crystal SiGeSn films with a Sn content as high as 25% [12]. Success in fabricating such compounds becomes possible as a result of the considerable degree of the replacement of Ge and Si atoms with Sn atoms under nonequilibrium conditions at low growth temperatures of 100–350°C.

The lattice constants of diamond-like Si–Ge–Sn alloys are consistent with Vegard's law; therefore, linear interpolation of the lattice constants between Si, Ge, and α-Sn makes it possible to obtain the lattice constant of the $Si_xSn_yGe_{1-x-y}$ ternary solution equal to that of elemental Ge. This circumstance is used in this study in order to investigate the initial stages of growth of $Si_xSn_yGe_{1-x-y}$ ternary alloys with the lattice constant of Ge. Previously, data were obtained on the initial stages of growth of GeSn binary alloys on Si (100) [13]. In this case, the growth of GeSn, as also the growth of pure Ge on Si (100), follows the Stranski–Krastanov mechanism.

In this study, we obtained the growth-temperature dependences for the critical thickness of the 2D–3D transition for $Si_xSn_yGe_{1-x-y}$ ternary alloys with a lat-

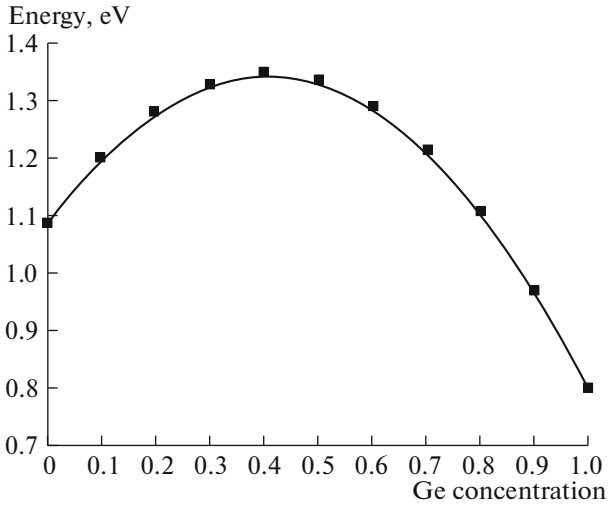

Fig. 1. Dependence of the width of the direct band gap for the SiGeSn ternary compound the lattice constant of which is equal to that of Ge.

tice parameter equal to that of elemental germanium; we also obtained statistical data on the size and density of Si–Ge–Sn islands in relation to the alloy composition in the range of growth temperatures 150–450°C.

2. EXPERIMENTAL

Heterostructures based on Si–Ge–Sn materials were grown under ultrahigh vacuum conditions (10^{-7} Pa) in a Katun' MBE installation equipped with an electron-beam evaporator for silicon and two Knudsen effusion cells for obtaining molecular beams of germanium and tin. Analytical equipment of the growth chamber includes a mass spectrometer, a quartz thickness meter, and a diffractometer of high-energy electrons (20 keV). We used *p*-Si (100) substrates. After chemical cleaning, the substrates were placed into the growth chamber, where the substrates were irradiated with a low-intensity flux of silicon at a temperature of 800°C for ~5 minutes until the (2 × 1) superstructure appeared. Then, a silicon buffer layer with a thickness of 40 nm was grown at a temperature of 700°C. The deposition rate of silicon amounted to ~0.35 Å/s. Growth of the Si–Ge–Sn layers on silicon was carried out at substrate temperatures in the range of 150–450°C. The rate of growth of germanium amounted to 0.09 Å/s, whereas the rates of silicon and tin varied from 0.018 to 0.072 Å/s and from 0.0045 to 0.018 Å/s, respectively.

The main in situ method for controlling the variation in the surface morphology was based on reflection high energy electron diffraction (RHEED). The RHEED patterns were recorded using a video camera during growth; after that, a profile along one of the crystallographic directions [110] or [100] was chosen and a variation in the intensity in space–time coordinates was made. The 2D–3D transition from a smooth surface to a surface with SiGeSn islands was determined from the variation in the profile-intensity distribution [14].

The morphology of the grown films was studied using the ex situ methods of scanning tunneling microscopy (STM) and atomic-force microscopy (AFM).

3. RESULTS AND DISCUSSION

The behavior of the lattice constant of ternary $Si_xSn_yGe_{1-x-y}$ alloys can be estimated from available data on binary systems [15]. In the case of the ratio of the silicon concentration to the tin concentration equal to four, the lattice constant of a ternary alloy equals the lattice constant of elemental germanium. We studied such ternary Si–Ge–Sn compounds whose lattice constant coincides with that of Ge.

We calculated the composition dependence of the electronic structure of the ternary $Si_xSn_yGe_{1-x-y}$ alloy using data reported in [16]. The dependence of the direct band gap in the $Si_xSn_yGe_{1-x-y}$ ternary alloy on the germanium concentration at values of silicon and tin concentrations such that the lattice constant of the ternary alloy equals that of germanium is shown in Fig. 1. The calculated values of the direct band gap vary in the range of 0.8–1.35 eV. Thus, it is shown that, at the same value of the lattice constant for the SiGeSn ternary alloy, one can obtain values of the band gap, which differ by more than 0.2 eV.

Films of the $Si_{4y}Sn_yGe_{1-5y}$ ternary alloy (the allowed values of y vary from 0 to 0.2) were grown by the method of low-temperature MBE at temperatures in the range of 150–450°C. The RHEED method was used to study the growth of these films. The diffraction patterns of the growth processes of germanium and the $Si_{4y}Sn_yGe_{1-5y}$ films are similar. A diffraction pattern from the flat surface of the wetting layer was observed first, then we observed the RHEED pattern corresponding to the onset of three-dimensional growth. We used the RHEED method during epitaxial growth to determine the critical thickness of the transition from two-dimensional to three-dimensional growth of the $Si_{4y}Sn_yGe_{1-5y}$/Si(100) structures as a function of the growth temperature.

The temperature dependence of the critical thickness of the 2D–3D transition at germanium concentrations of 60 and 80% is nonmonotonic and features a maximum. Qualitatively, such behavior can be accounted for by a change in the mechanism of two-dimensional growth. Figure 2 schematically represents variations in the mechanisms of two-dimensional growth; also, for the sake of comparison, we show the temperature dependence of the critical thickness of the 2D–3D transition for the growth of pure germanium on a Si (100) surface [17]. At low temperatures,

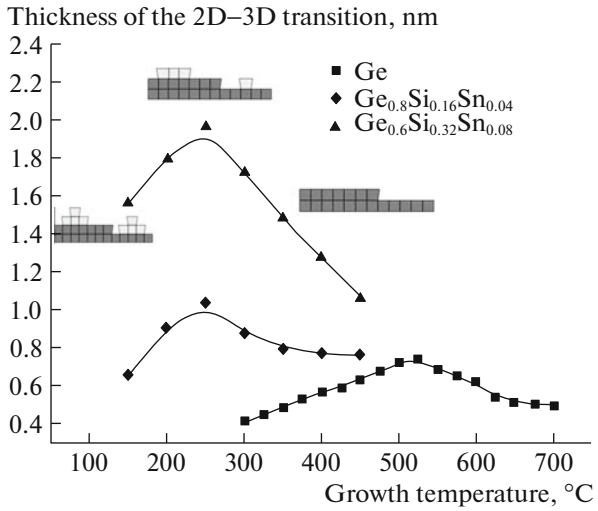

Fig. 2. Temperature dependence of the critical thickness corresponding to the 2D–3D transition in the case of the epitaxial growth of $Si_{4y}Sn_yGe_{1-5y}$ on Si (100).

adatoms, due to their low mobility, cannot reach the edge of 2D islands, which grow further and fill the next layer on the surface of the island. Then, multilevel islands are transformed into three-dimensional islands and give rise to a high surface roughness. As the growth temperature is increased, the density of multilevel islands (and, as a consequence, the surface roughness) decreases; as a result, the critical thickness of the 2D–3D transition increases. Figure 3 shows the variation in the intensity profile of the diffraction pattern in the [110] azimuth along the direction of mirror reflection during the course of growth of the $Si_{0.16}Sn_{0.04}Ge_{0.8}$ layer at a temperature of 150°C. In this

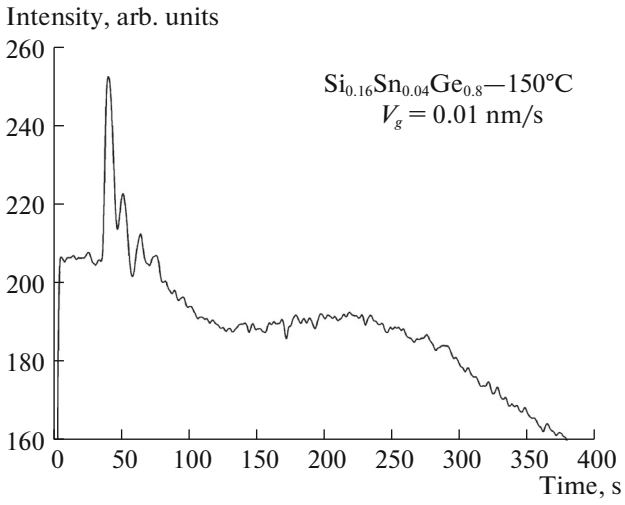

Fig. 3. Variation in the intensity of the mirror reflection in the RHEED pattern during growth of the $Si_{0.16}Sn_{0.04}Ge_{0.8}$ structure at a temperature of 150°C.

case, we observed oscillations in the intensity of the mirror reflection. The presence of oscillations confirms that epitaxial growth proceeds according to the two-dimensional island mechanism.

As the growth temperature is increased, the critical thickness of the 2D–3D transition decreases as a result of a decrease in the degree of film relaxation. A transition of the mechanism of growth occurs due to the motion of atomic steps, which is confirmed by a lack of oscillations of the mirror reflection during growth.

The transition between growth mechanisms for ternary $Si_{4y}Sn_yGe_{1-5y}$ compounds occurs at a lower temperature compared with the process of growth of Ge on Si (100). As the tin concentration is increased in the ternary compound, the critical thickness of the 2D–3D transition increases. A decrease in the temperature of the transition between growth processes and an increase in the critical thickness for the 2D–3D transition are related to the presence of tin, which acts as a surfactant, promotes the surface diffusion of adatoms, and segregates at the surface of the growing film [18].

The process of the heteroepitaxial growth of Ge films on Si (100) qualitatively corresponds to the growth process of the ternary $Si_{4y}Sn_yGe_{1-5y}$ alloy. The features of variations in the diffraction pattern indicate that the morphologies of the surface layers of the ternary $Si_{4y}Sn_yGe_{1-5y}$ alloy and of Ge qualitatively coincide. The known morphological states were observed: a wetting layer and 3D islands on this layer. The (2 × 1) and (2 × N) superstructures are present in both cases on the surface of the wetting layer. The period N varied in relation to the composition of the ternary alloy and the thickness of the epitaxial film. During the course of deposition of the $Si_{4y}Sn_yGe_{1-5y}$, the period N changed from 14 to 6; simultaneously, the (2 × 1) superstructure disappeared, which was not observed in the case of the growth of Ge on Si (100) (apparently, this is related to the accumulation of tin on the surface). As the thickness of the epitaxial film is further increased, the (5 × 1) superstructure is formed on the surface of the wetting layer. Such a reconstruction was observed [19, 20] for the Sn/Si (100) system. As the growth temperature is decreased from 350 to 200°C, the (5 × 1) structure degenerates and the (2 × 1) and (2 × N) superstructures appear. Such behavior of the surface structure is possibly indicative of a decrease in the effect of tin segregation as the growth temperature is lowered.

The STM and AFM methods were used to obtain images of the surface of ternary $Si_{4y}Sn_yGe_{1-5y}$ compounds; we analyzed these images in the region of three-dimensional growth. SiGeSn islands are observed on the surface. We obtained the dependences of the average size and density of islands at various growth temperatures and for different compositions of the ternary $Si_{4y}Sn_yGe_{1-5y}$ alloy. Figure 4 shows the STM image of the $Si_{0.32}Sn_{0.08}Ge_{0.6}$ film grown at a

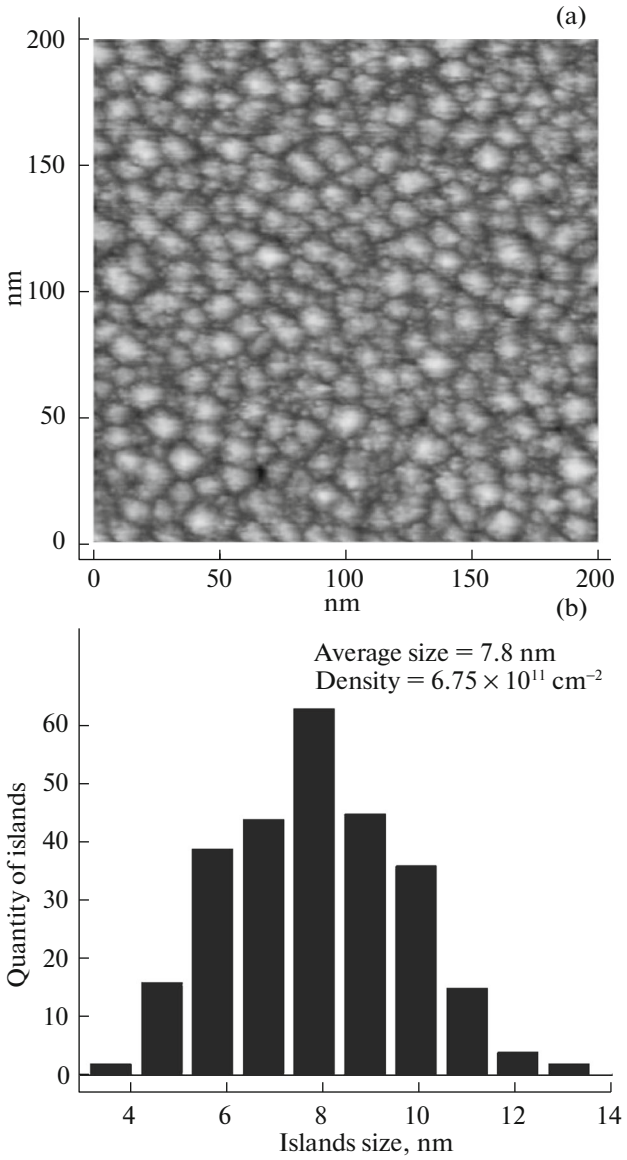

Fig. 4. (a) STM image of a $Si_{0.32}Sn_{0.08}Ge_{0.6}$ film 2.4-nm thick grown at a temperature of 250°C. (b) The distribution of the number of islands in relation to the size of the island base for the $Si_{0.32}Sn_{0.08}Ge_{0.6}$ structure grown at a temperature of 250°C.

temperature of 250°C and the distribution of the number of islands in relation to the size of the island base.

In order to determine the effects of the composition and growth temperature on the properties of an array of SiGeSn nanoislands, we constructed the dependence of the island sizes on the growth temperature and the composition of the $Si_{4y}Sn_yGe_{1-5y}$; this dependence is presented in Fig. 5. It is shown by analysis of the AFM and STM images that, as the growth temperature is increased, the size of the island base becomes larger and, correspondingly, the island density decreases. The increase in the island sizes is

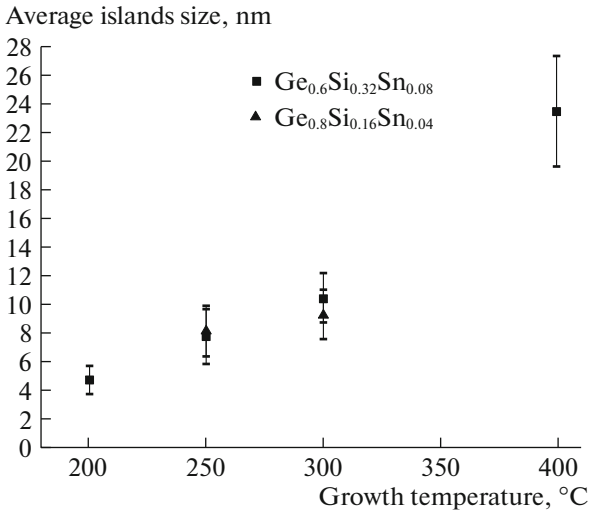

Fig. 5. The distribution of sizes of $Si_{4y}Sn_yGe_{1-5y}$ islands in relation to the growth temperature.

related to the fact that, as the growth temperature is increased, the diffusion of atoms over the surface is stimulated; the same is true for the incorporation of atoms into the islands. It is worth noting that the sizes of the islands grown at temperatures of 250 and 300°C are practically identical, in spite of the fact that the germanium concentration in the ternary alloy differs by 20%.

The STM data were used to obtain the ratio of the island height to the transverse size in relation to the transverse size for the $Si_{4y}Sn_yGe_{1-5y}$ alloys grown at a temperature of 250°C. Such a ratio (however, for germanium quantum dots) was widely described in available publications [21]. For pre-pyramids and hut-clusters, the ratio of the sizes equals approximately 0.05–0.15. GeSiSn islands grown at a temperature of 250°C feature a similar relation of sizes (0.06–0.14).

4. CONCLUSIONS

It is established in this study that the process of growth of thin films of $Ge_{1-5y}Si_{4y}Sn_y$ on Si (100) occurs via the Stranski–Krastanov mechanism. We determined the specific features of the growth of $Ge_{1-5y}Si_xSn_y$ layers whose lattice constant coincides with that of elemental germanium. In contrast to Ge and GeSn films, in the case of the epitaxial growth of the ternary $Ge_{1-x-y}Si_xSn_y$ compound on Si (100), we observed the decay of the (2 × 1) superstructure with its further disappearance and a change in the periodicity N in the superstructure (2 × N) from 14 to 6 and the formation of the (5 × 1) superstructure.

We analyzed variations in the intensity of reflections in the RHEED pattern during the growth of $Ge_{1-5y}Si_{4y}Sn_y$ ternary alloys on Si (100) and obtained the temperature dependence of the critical thickness

corresponding to the 2D–3D transition in the range of growth temperatures 150–450°C. This dependence at germanium concentrations of 60 and 80% is nonmonotonic, is similar to that in the case of the growth of pure Ge on Si (100), and is caused by a change in the mechanism of growth (from the two-dimensional island mechanism of growth to the mechanism of growth by atomic steps). The change in the growth mechanisms is confirmed by the presence and absence of oscillations in the mirror reflection during the growth of the $Si_{0.16}Sn_{0.04}Ge_{0.8}$ ternary compound at temperatures of 150 and 350°C, respectively. The observed shift of the extremum point to lower temperatures is attributed to the effect of tin (as a surfactant) stimulating surface diffusion.

Using STM and AFM methods, we obtained the dependence of the average size of the nanoislands in the region of three-dimensional growth on the composition of a ternary alloy and growth temperature. As the growth temperature is increased from 200 to 400°C, the average size of the nanoislands increases from 4.7 to 23.6 nm. The ratio of the height to the lateral size of the $Ge_{0.8}Si_{0.16}Sn_{0.04}$ and $Ge_{0.6}Si_{0.32}Sn_{0.08}$ nanoislands synthesized at a substrate temperature of 250°C is in the region of 0.06–0.14, which corresponds to the size distribution for hut-clusters of Ge upon its epitaxy on the surface of Si (100).

REFERENCES

1. R. A. Soref, J. Kouvetakis, J. Tolle, J. Menendez, and V. D'Costa, J. Mater. Res. **22**, 3281 (2007).
2. V. R. D'Costa, Y. Y. Fang, J. Tolle, J. Kouvetakis, and J. Menendez, Phys. Rev. Lett. **102**, 107403 (2009).
3. R. A. Soref, J. Vac. Sci. Technol. A **14**, 913 (1996).
4. G. Sun, H. H. Cheng, J. Menendez, J. B. Khurgin, and R. A. Soref, Appl. Phys. Lett. **90**, 251105 (2007).
5. G. Sun, R. A. Soref, and H. H. Cheng, Opt. Express **19**, 19957 (2010).
6. R. T. Beeler, D. J. Smith, J. Kouvetakis, and J. Menendez, IEEE J. Photovolt. **2**, 434 (2012).
7. Y. Y. Fang, J. Xie, J. Tolle, R. Roucka, V. R. D'Costa, A. V. G. Chizmeshya, J. Menendez, and J. Kouvetakis, J. Am. Chem. Soc. **130**, 16095 (2008).
8. J. Werner, M. Oehme, M. Schmid, M. Kaschel, A. Schirmer, E. Kasper, and J. Schulze, Appl. Phys. Lett. **98**, 061108 (2011).
9. J. Kouvetakis, J. Menendez, and A. V. G. Chizmeshya, Ann. Rev. Mater. Res. **36**, 497 (2006).
10. S. Wirths, R. Geiger, N. von den Driesch, G. Mussler, T. Stoica, S. Mantl, Z. Ikonic, M. Luysberg, S. Chiussi, J. M. Hartmann, H. Sigg, J. Faist, D. Buca, and D. Grutzmacher, Nature Photon. **9**, 88 (2015).
11. O. Gurdal, P. Desjardins, J. R. A. Carlsson, N. Taylor, H. H. Radamson, J.-E. Sundgren, and J. E. Greene, J. Appl. Phys. **83**, 162 (1998).
12. M. Oehme, K. Kostecki, M. Shmid, F. Oliveira, E. Kasper, and J. Schulze, Thin Solid Films **557**, 169 (2014).
13. V. I. Mashanov, V. V. Ulyanov, V. A. Timofeev, A. I. Nikiforov, O. P. Pchelyakov, I.-S. Yu, and H. H. Cheng, Nanoscale Res. Lett. **6**, 85 (2011).
14. A. I. Nikiforov, V. A. Cherepanov, and O. P. Pchelyakov, Mater. Sci. Eng. B **89**, 180 (2002).
15. P. Aella, C. Cook, J. Tolle, S. Zollner, A. V. G. Chizmeshya, and J. Kouvetakis, Appl. Phys. Lett. **84**, 888 (2004).
16. V. R. D'Costa, C. S. Cook, J. Menedez, J. Tolle, J. Kouvetakis, and S. Zollner, Solid State Commun. **138**, 309 (2006).
17. A. I. Nikiforov, V. V. Ulyanov, V. A. Timofeev, and O. P. Pchelyakov, Microelectron. J. **40**, 782 (2009).
18. A. E. Dolbak and B. Z. Olshanetsky, Centr. Eur. J. Phys. **6**, 634 (2008).
19. K. Ueda, K. Kinoshita, and M. Mannami, Surf. Sci. **145**, 261 (1984).
20. M. Pedio and A. Cricenti, Surf. Sci. **374**, 251 (1997).
21. A. Vailionis, B. Cho, G. Glass, P. Desjardins, D. G. Cahill, and J. E. Greene, Phys. Rev. Lett. **85**, 3672 (2000).

Translated by A. Spitsyn